Korean J. Chem. Eng., **27**(4), 1296-1300 (2010)
DOI: 10.1007/s11814-010-0178-7

Physical and thermal properties of acid-graphite/styrene-butadiene-rubber nanocomposites

Sung Ho Song†, Ho Kyun Jeong, Yong Gu Kang, and Chun Taek Cho

NEXEN Tire corporation R&D Center, 30, Yusan-dong, Yangsan-si, Gyeongnam 626-230, Korea
(*Received 26 June 2009 • accepted 10 November 2009*)

Abstract−In general, carbon-based materials play a major role in today's science and technology and are required to advance with better properties to meet new requirements or to replace existing materials. We fabricated rubber composites reinforced with 5-weight% acid-graphite. The structural, mechanical and thermal properties of these composites were studied and compared. XRD studies indicated that the structure of the acid treated pristine-graphite (acid-graphite) did not change that of pristine graphite. Tensile properties of the composites indicated higher modulus, tensile strength and elongation in comparison with composites of pristine graphite, carbon black. Also, the composites were found to be in improving tendency with thermal properties and fatigue properties. The acid-graphite was investigated for surface morphology by scanning electron microscopy (SEM) and defects or purity by Raman spectroscopy. In this article, we discuss the influence of acid-graphite on rubber with high mechanical and thermal properties.

Key words: Acid Graphite, Styrene-butadiene-rubber

INTRODUCTION

In recent years, polymer based nanocomposites reinforced with graphite-nanoplates have shown substantial improvement in mechanical, electrical conductivity and barrier properties over the unmodified polymer [1-7]. These excellent properties may be enhanced at the nanoscale if graphite can be separated down to that plane to a nanometer thickness [8]. They would form high aspect ratio and high modulus graphite nanosheets. Furthermore, the graphite nanosheets could have an enormous surface area because both sides of the sheets are accessible. Therefore, the dispersion of such nanosheets in a matrix will play a key role in the improvement of both physical and thermal properties of the resultant nanocomposites.

There are no reactive ion groups on the graphite layers. It is difficult to incorporate organic molecules or rubbers directly into the interlayer of graphite through an ion exchange reaction to prepare the rubber/graphite composites. Therefore, pristine graphite is first converted to intercalated or expandable graphite through chemical oxidation in the presence of concentrated HNO_3 acid. And then a coupling agent is added to facilitate both physical and chemical interactions between acid treatment graphite and rubber. In other words, we proposed a modified expandable graphite to achieve homogeneous nanodispersion and to increase the reinforcement of graphite in rubber matrix.

Recently, several groups [9-12] reported their work on blending the expanded graphite with polymer via either the in situ polymerization or the solution compounding to achieve nanocomposites of polymer with graphite. The results reported were significant in that a markedly low volume fraction of expanded graphite was needed to satisfy the percolation threshold of conductivity in the as-prepared PMMA [9], nylon-6 [10], PS [11] and PS-PMMA [12].

However, there are not many studies on fabrication methods of rubber-based graphite nanocomposites and their influence on physical and thermal properties.

Therefore, we used modified expandable graphite to reinforce styrene butadiene rubber (SBR) in the present work. SBR is a high performance rubber with a combination of excellent mechanical properties, abrasion resistance, adhesion to fabrics and thermal aging resistance, which can be used in many diverse applications.

In this work, we fabricated composites that contain reinforcing graphite platelets in the SBR matrix and evaluated their morphology, curing, physical, thermal and fatigue properties.

EXPERIMENTAL

1. Materials

The matrix material was a styrene butadiene rubber (SBR) from Kumho Petrochem. The SBR1500 consisted of 23% styrene and 77% butadiene. The chemical structure of this material is shown in Fig. 1. The reinforcing particles were pristine graphite supplied by Timcal. The properties of the as-received graphite platelets are summarized in Table 1. This graphite consists of thin hexagonal plates or distorted clusters of flaky plates from the SEM image. It was difficult to measure the thickness of as-received graphite platelets from SEM. The surface area of pristine graphite is ~8.6 m^2/g as measured by gas adsorption technique (BET), and the thickness was cal-

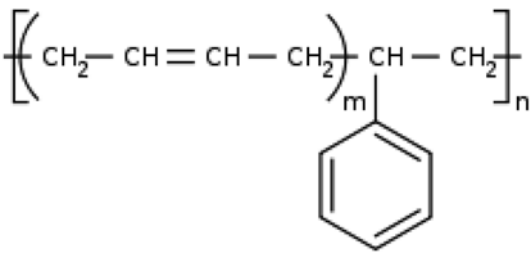

Fig. 1. The chemical structure of styrene butadiene rubber.

†To whom correspondence should be addressed.
E-mail: sh.song@nexentire.co.kr

Table 1. Properties of graphite platelets

Composition	Carbon
Color	Dark gray to black
Scott density (g/cm^3)	0.23
Surface area BET (m^2/g)	8.6
Oil adsorption (DBP)	112
Mean particle size (μm)	22

culated by using the formula,

$$A=2/\rho t \quad (1)$$

Where, A is the specific surface area per unit mass, m^2/g; ρ is the density, g/cc; t is the platelet thickness, nm.

The thickness of as-received graphite platelets was as high as 1,011 nm when calculated from Eq. (1).

2. Sample Preparation

Acid-graphite flakes were chemically prepared by HNO_3 treatment (Graphite/HNO_3=1 g/10 ml). Briefly, a concentrated HNO_3 was mixed with graphite flakes at room temperature and stirred continuously for 18 h. The acid-graphite was then washed thoroughly with water until the solution became neutral, and dried at 100 °C to remove the remaining moisture. The surface area of acid-graphite is ~10.6 m^2/g, and the thickness was as high as 820 nm from Eq. (1). This means that the specific surface area is broader and the thickness of acid-graphite is thinner than that of natural graphite by the acid-treatment.

Generally, it is also reported that the acid treatment of natural graphite generates oxygen containing functional groups (-OH and -COOH) that facilitate both physical and chemical interactions between graphite and polymer [12,13].

3. Composition Fabrication

The graphite/SBR composites were prepared following standard procedures. First, the SBR was mixed with 50 phr (parts per hundred rubber by weight) carbon black in a banbury mixer. And then, the SBR compounds with 5 phr pristine-graphite, acid-graphite, carbon black and 0.8 phr coupling agent were prepared. The additives and vulcanization agent were added at the end since it helped to start the curing process of the mixture. The compounds were placed in the aluminum mold and cured at 160 °C for T_{90} by rheometer under pressure. The formulations of the graphite/SBR composites are summarized in Table 2.

Table 2. Formulation of the graphite platelet/SBR composites

(Unit: phr)

	1 Control	2 C/B	3 P/G	4 A/G	5 P/C	6 A/C
SBR	100	100	100	100	100	100
Pure-graphite	-	-	5	-	5	-
Acid-graphite	-	-	-	5	-	5
Coupling agent	-	-	-	-	0.8	0.8
ZnO	3	3	3	3	3	3
Stearic acid	1	1	1	1	1	1
Carbon black	50	55	50	50	50	50
Sulfur	1.75	1.75	1.75	1.75	1.75	1.75
TBBS	1	1	1	1	1	1

4. Characterization and Measurements

Scanning electron microscopy (SEM, JEOL JSM-6490LV) was used to observe the morphology of the graphite platelets. Since graphite is conductive, the particles could be examined at 20 KV accelerating voltage without gold coating. X-ray diffraction was used to verify the structure of the graphite platelets. X-ray measurements were conducted on an X-ray diffractometer Bruker, Germany using CuKα radiation at 40 KV and 40 mA. The scanning range was 10-80° with a scanning speed of 5°/min. Raman spectroscopy was mainly used to verify the nature of the graphite and the overall homogeneity of the sample. The Raman spectra, obtained in the range 1,000-2,000 cm^{-1}, show a band at 1,588 cm^{-1} (G-band) due to the vibration mode, and a band at 1,357 cm^{-1} (D-band) arising from the disordered-induced mode.

The electrical resistance of these manufactured composites was examined using the two-prove method in the TERAOHM, MI2077 at room temperature, and the thermal conductivity was characterized by thermal conductivity analyzer (QTM-500).

Curing characteristics were measured over 30-min period at 160 °C using a moving-die rheometer (DRM-100(LP-171)). Tensile tests were carried out in an Instron tensile machine (Intron Co., UK) at a crosshead speed of 300 mm/min. The dumbbell-shaped samples were 100 mm in length, 1 mm in thickness and 5 mm in width. At least four tests were carried out for each case.

Shore A hardness was measured by using a hand-held shore A durometer according to TECLOCK. The fatigue properties of composites were characterized by using Demmattia (UESHIMA).

RESULTS AND DISCUSSION

1. Materials Characterization

Table 3 shows the Raman spectroscopy of pristine-graphite and acid-graphite. The main features in the Raman spectroscopy of graphite are the so-called G and D bands, which lay at around 1,560 and 1,360 cm^{-1} respectively. The G band of the acid-graphite appeared almost the same as that of the pristine-graphite, but the acid-graphite demonstrated an increased D-band. In other words, the I(D)/I(G) ratio of acid-graphite is higher than that of pristine-graphite. Since the D-band is proportional to the defects of graphite, this result indicates significant devastation of acid-graphite. The acid treatment of pristine-graphite generates functional groups that facilitate both physical and chemical interactions between graphite and polymer.

Fig. 2 shows the powder XRD pattern of pristine-graphite and acid-graphite. The XRD profiles are dominated by peaks at 26° and 54°, of the same intensity in the samples, which is characteristic of highly structured graphite carbon (002) and (004). Also, a weak peak and a shoulder were observed at 42.5° and 44°, indicating (100) and (101) graphene layers, respectively. Corresponding to (101) and (012) reflection, the additional peaks are also indexed to a rhombo-

Table 3. Raman spectroscopy results of pure-graphite and acid-graphite

	D-band	G-band	I(D)/I(G)
Pristine-graphite	0.00206	0.00099	208%
Acid-graphite	0.00240	0.00091	264%

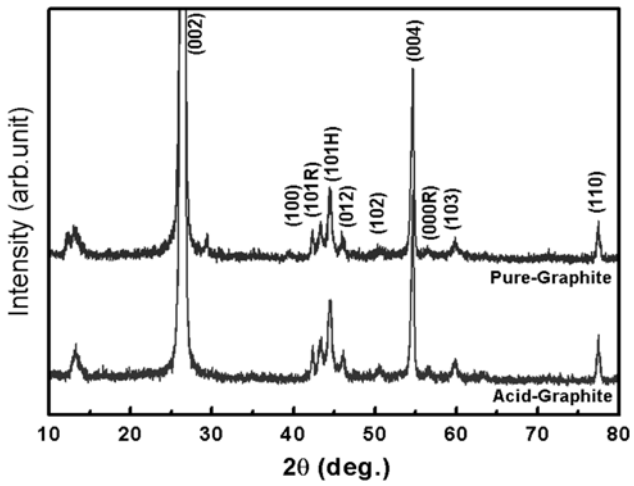

Fig. 2. XRD patterns of pristine-graphite and acid-graphite.

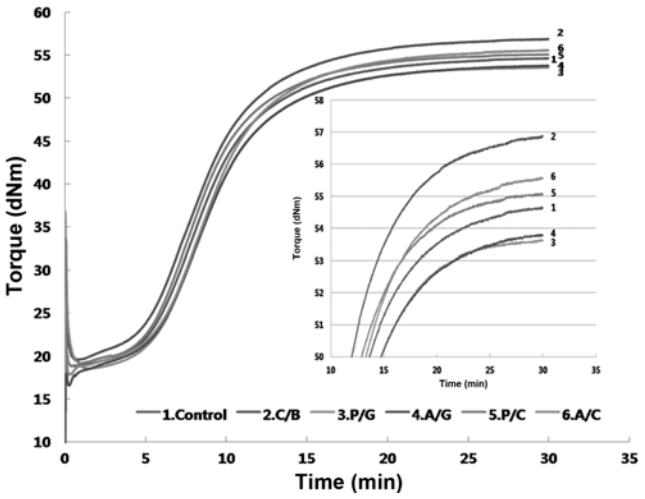

Fig. 4. Curing curves of graphite/SBR compound at 160 °C.

hedral phase of graphite. The acid-treatment does not substantially modify the crystallographic properties of the graphite.

The pristine-graphite and acid-graphite were examined by SEM and are shown in Fig. 3. Graphite samples consist of thin polygon plates and disordered clusters of flaky plates. But, acid-graphite is more finely smashed than pristine-graphite and has a crinkled paper shape, consisting of balloon segments. The specific surface area of the graphite is increased from 8.6 m^2/g to 10.6 m^2/g, but thickness is thinner than from 1,011 nm to 820 nm by acid treatment.

2. Characterization of Graphite/Rubber Composites

The curing curves of graphite/rubber composites are shown in

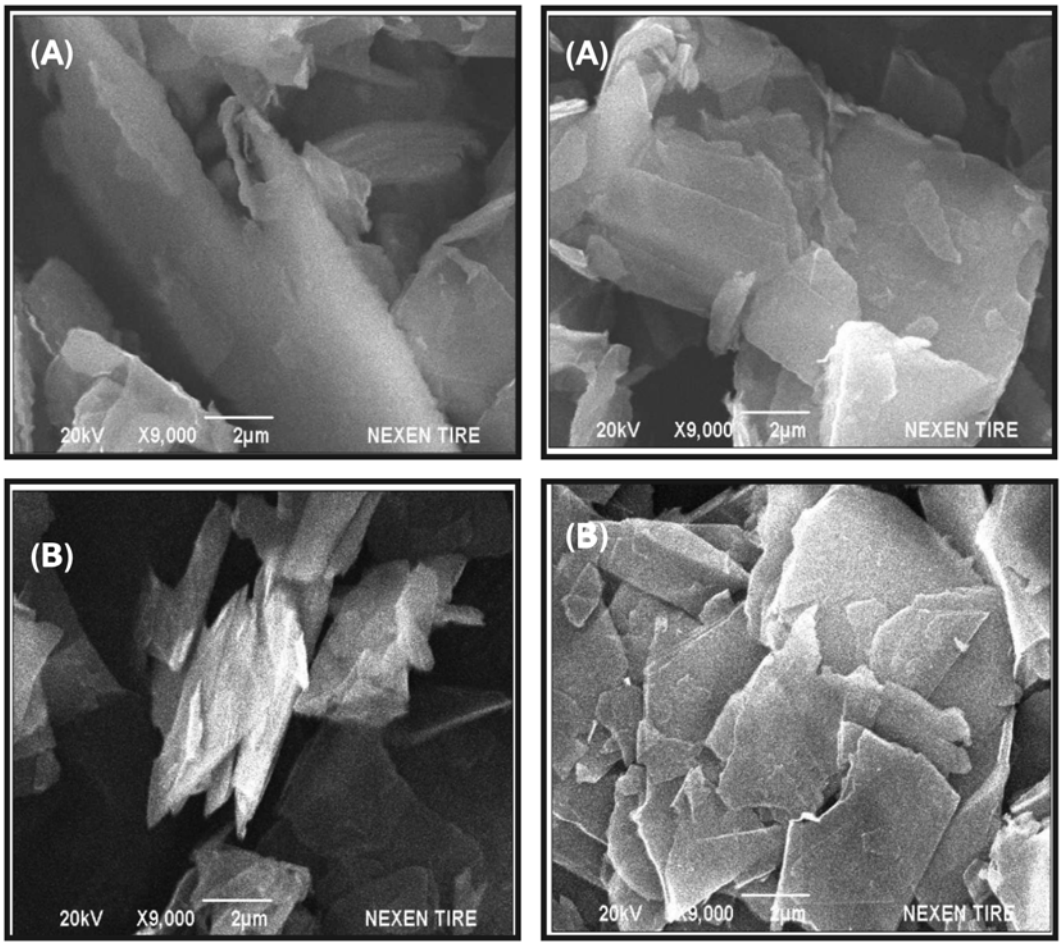

Fig. 3. SEM image of graphite (A) Pristine-graphite (B) Acid-graphite.

Table 4. Curing characteristics of graphite/SBR composites

	1 Control	2 C/B	3 P/G	4 A/G	5 P/C	6 A/C
T_{40} (min)	8.1	7.5	8.1	7.8	7.8	7.5
T_{90} (min)	15.0	14.6	14.9	14.8	14.7	14.3
Min Torque (M_L, dNm)	19.1	19.6	18.6	16.6	18.8	17.8
Max Torque (M_H, dNm)	54.6	56.9	53.6	53.8	55.1	55.6
Δ Torque	35.5	37.3	35	37.2	36.3	37.8

Table 5. Hardness and tensile properties of graphite/SBR composites

	1 Control	2 C/B	3 P/G	4 A/G	5 P/C	6 A/C
Hardness	71.0	72.0	72.0	74.0	73.0	74.0
300%-Modulus (MPa)	21.9	26.3	22.5	22.6	23.1	25.3
Tensile strength (MPa)	25.7	26.9	27.7	29.0	28.3	30.0
Elongation (%)	342.0	341.0	371.0	397.0	381.0	395.0

Fig. 4 and some parameters of curing properties are reported in Table 4. Three regions are observed in Fig. 4. The first region is the scorch delay or induction period where the torque of compounds decreased. The second region is where the curing reaction occurred. The network structure was formed in this period, leading to the sharp increment of the torque. In third region, curing curves reached to a plateau when the network was matured by equilibrium. The cure time of rubber composite using acid-graphite and coupling agent (A/C) is faster than other rubber composites. The reason for the shorter cure time of the rubber composite using A/C is probably due to the increase of thermal transition of SBR in the presence of A/C which could promote the fulfillment of vulcanization. That is, the A/C increases the specific surface by the acid treatment, and then the thermal transition of the composite using A/C is improved by increasing the filler-filler and filler-matrix interactions.

M_L is the lowest torque and M_H is the highest torque at curing curves. M_H-M_L represents the crosslink density of vulcanization. M_H-M_L slightly increases after loading A/C. This indicates that the addition of A/C has little effect on the crosslink density of rubber vulcanization.

The hardness and the tensile properties of graphite composites are summarized in Table 5. From this table, shore A hardnesses of the composites are slightly increased, indicating that small additions of filler do not largely influence the rubber matrix. The composite reinforced with A/C showed about 15% increase over control and about 12% increase over P/G in modulus. And incorporation of A/C in SBR leads to an increase in both tensile strength and elongation at break. The tensile strength of the A/C composite increased roughly 15% and the elongation also increased approximately 15% compared with the control. It is obvious that A/C has a great reinforcing effect on SBR with respect to small filler loadings.

The reason why mechanical property is increased is that the specific surface area is higher and the physical and chemical interaction between graphite and polymer is facilitated.

The fatigue properties of graphite/rubber composites are shown in Table 6.

Table 6. Fatigue properties of graphite/SBR composites

(Unit: cm)

	1 Control	2 C/B	3 P/G	4 A/G	5 P/C	6 A/C
2000 회	5.02	8.03	5.45	5.28	5.90	5.26
6000 회	9.82	14.36	9.55	8.66	9.06	9.47
10000 회	13.88	18.43	11.27	9.91	11.36	11.66
dc/dn	4.74	6.56	4.23	3.74	4.17	4.15

Table 7. Thermal properties of graphite/SBR composites

(Unit: W/mK)

	1 Control	2 C/B	3 P/G	4 A/G	5 P/C	6 A/C
Thermal conductivity	0.3092	0.3101	0.3311	0.3425	0.3444	0.3694

Fatigue crack growth (dc/dn) of A/G is lower than of any other composites.

$$dc/dn = AG^{\alpha} \quad (2)$$

Where, c is the crack length, n is the cycles, G is the tear energy.

This equation means that fatigue crack growth is proportional to the tear energy and indicates that the tearing energy is decreased and fatigue life is increased from Eq. (2). Generally, several groups proposed that good dispersion and complete exfoliation are achieved by a combination of both synthesis and processing techniques. The synthesis of expanded graphite as well as graphite nanosheets is well documented in the literature [1,5,12]. Accordingly, we estimate that it is probably that fatigue crack growth of composite using acid-graphite is decreased because the acid-graphite is uniformly dispersed in SBR due to the functional groups.

Thermal properties of graphite/rubber composites are shown in Table 7. Thermal conductivity of A/C is higher than that of any other composites, and is increased approximately 19% compared with control.

Therefore, the reasons which are increased thermal conductivity of A/C are increased the specific surface area and improved the interactions between rubber and graphite.

The reason is that the specific surface area is increased, wherefore the interactions between rubber and graphite are enhanced.

CONCLUSIONS

Graphite/SBR composites were prepared and their mechanical, thermal and fatigue properties were evaluated according to the fillers. The acid graphite of large surface area did not substantially modify the crystallographic properties and was more finely smashed. The addition of acid-graphite into the SBR was shorter curing time and had a remarkable effect on the physical properties. The tensile strength of the A/C composite increased roughly 15% and the elongation also increased approximately 15%. In fatigue properties, fatigue crack growth of composite using acid-graphite was decreased because the acid-graphite is uniformly dispersed in SBR due to the functional groups. And the thermal conductivity of A/C was also

higher than any other composites, about 19%. In other words, curing, physical, thermal and fatigue properties which were originated by A/C were highly improved due to wide specific surface and to facilitate both physical and chemical interactions between graphite and polymer and to disperse in SBR.

REFERENCES

1. L. T Drzal and H. Fukushima, *Am. Chem. Soc., Div. Polym. Chem.*, **42**(2), 42 (2001).
2. A. Yasmin, J. J Luo and M. I. Daniel, *Composites Sci. Technol.*, **66**, 1182 (2006).
3. I. M. Afanasov, V. A. Morozov, A. V. Kepman, S. G. Ionov, A. N. Seleznev, G. Van Tendeloo and V. V. Avdeev Preparation, *Carbon*, **47**, 263 (2009).
4. M. R. Cuervo, A. N Esther, E. Diaz, S. Ordonez, A. Vega, A. B. Dongil and R. R Inmaculada, *Carbon*, **46**, 2096 (2008).
5. G. Chen, W. Weng, D. Wu and C. Wu, *European Polymer Journal*, **39**, 2329 (2003).
6. A. Yasmin and I. M. Daniel, *Polymer*, **45**, 8211 (2004).
7. N. A. Kotov, *Nature*, **442**(7100), 254 (2006).
8. S. Stankovich, D. A. Dikin, R. D. Piner, K. A. Kohlhaas, A. Kleinhammes, Y. Jia, Y. Wu, S. T. Nguyen and R. S. Ruoff, *Carbon*, **45**, 1558 (2007).
9. H. Kim, H. T. Hahn, L. M. Viculis, S. Gilje and R. B. Kaner, *Carbon*, **45**, 1578 (2007).
10. Y. X. Pan, Z. Z. Yu, Y. C. Ou and G. H. Hu, *J. Polym. Sci., Part B: Polym. Phys.*, **38**, 1626 (2000).
11. M. Xiao, L. Sun, J. Liu, Y. Li and K. Gong, *Polymer*, **43**, 2245 (2002).
12. G. Chen, C. Wu, W. Weng, D. Wu and W. Yan, *Polymer*, **44**, 1781 (2003).
13. W. Zheng and S. C. Wong, *Composites Sci. Technol.*, **63**, 225 (2003).
14. J. W Shen, X. M Chen and W. Y. Haung, *J. Appl. Polym. Sci*., **88**, 1864 (2003).
15. M. A. Lopez-Manchado, J. Biagiotti, L. Valentini and J. M. Kenny, *J. Appl. Polym. Sci*., **92**, 3394 (2004).